Power Efficient Wireless LAN Using 16-State Trellis-Coded Modulation for Infrared Communications

Hae Geun Kim

School of Computer and Information Communication,
Catholic University of Daegu,
330 Kumrak-ri, Hayang-up, Kyungsan-si, 712-702, Korea
kimhg@cu.ac.kr

Abstract. Optical wireless communication employing 16-state trellis-coded multiple-subcarrier modulation with a fixed bias is introduced, where 4-dimensional vectors having the largest Euclidean distance for 32 signal points are used. After combining coding with the 4-dimensional modulation, the proposed system improves the power and the bandwidth efficiency, significantly. The performance evaluation results are that the normalized power and the bandwidth requirements are reduced up to 6.1 dB and 5.8 dB compared to those of the block codes using QPSK, respectively. The proposed system needs much less power and bandwidth than the counterparts transmitting the same bit rates for optical wireless connection.

1 Introduction

A Wireless Local Area Network (WLAN) provides over the air interface standardized in IEEE 802.11 that includes two different technologies based on infrared and radio frequency (RF) for the physical layer [1]. Infrared wireless local access links offers a virtually unlimited bandwidth at low cost because optical sources and receivers are capable of high-speed operation.

When an optical WLAN is used for indoor use there are two major challenges that are the scattering of the light by the interior of room and power efficiency. To overcome those issues, Multiple-Subcarrier Modulation (MSM) systems with Intensity Modulation / Direct Detection (IM/DD) in optical wireless communications are popularly researched [2], [3], [4]. IM/DD MSM systems are attractive not only for minimizing inter-symbol interference (ISI) on multi-path channels between narrowband subscribers, but also for providing immunity to ambient light inducing in an infrared receiver. Yet, the efficiency of average optical power intensity is poor as the larger number of subcarriers in an MSM system.

In this paper, the MSM for infrared wireless communications using 16-state trellis-coded modulation (TCM) [7] is introduced where the newly generated 4-Dimensional (4-D) vectors for 32 signal symbols with the maximized minimum distances are employed. The block coder of the proposed system including a 4/5 convolutional

M. Gavrilova et al. (Eds.): ICCSA 2006, LNCS 3982, pp. 104 – 114, 2006.

encoder and an impulse generator maps the information bits to be generated to the symbol amplitudes modulated on to the subcarriers. The computer derived 4-D vectors for 32 symbols are symmetrically constructed on the surface of a 4-D sphere. Also the fixed bias is used for all symbols so that the power used for each symbol is constant and equals the average transmitted power. In the proposed system, one symbol is transmitted with 4 orthogonal subcarrier signals, while one symbol is transmitted with one subcarrier in conventional On-OFF Keying (OOK) and with two subcarriers in Quadrature Phase Shift Keying (QPSK). The performance evaluation for each scheme is carried out, and the power and bandwidth requirements of the proposed system are compared with that of the three block coders using QPSK scheme as counterparts.

2 4-D IM/DD MSM System in Optical Channel

Fig. 1 depicts the transmitter and receiver design used in the proposed MSM transmission scheme with 4-D orthogonal modulation where the transmitter in Fig. 1 (a) transmits Nk information bits during each symbol interval of duration T. In the block coder of each 4-D MSM in Fig. 1 (b), k input bits are encoded by $k/k+1$ convolutional encoder. The $k+1$ encoder output bits are transformed into one of M symbols, $\boldsymbol{A}_i$, where $M = 2^{k+1}$ and, $i = 0, \ldots, M$, then, each symbol A_i is mapped to a corresponding vector of 4-D symbol amplitudes, $\boldsymbol{a}_i = (a_{i1}, a_{i2}, a_{i3}, a_{i4})$. In the proposed system, $k = 4$ is chosen, so 32 symbols are generated for each 4-D MSM.

Since the electrical MSM signal $s(t)$ can be negative or positive, a baseband dc bias $b(t)$ must be added. After optical modulation using a LED or a LD, the MSM optical output in Fig. 1 (a) can be expressed as $x(t) = A[s(t) + b(t)] \geq 0$ where A is a nonnegative scale factor. The average optical power is $P = AE[s(t)] + AE[b(t)]$ where $E[x]$ represents an expected value of x.

If the subcarrier frequency $\omega_n = n(2\pi/T)$ and $g(t)$ is used in the MSM, $E[s(t)]$ is always 0 and the optical power P only depend on $b(t)$. Hence the average optical power can be given by $P = AE[b(t)]$. When the bias signal is properly chosen, the average power requirement of the MSM system can be decreased.

For fixed bias, the bias has the same magnitude with the smallest allowable value of electrical MSM signal $s(t)$ given by $b_0 = -\min_t s(t)$. For time-varying bias, the bias has the smallest allowable symbol-by-symbol value. In general, the average optical power with time-varying bias is smaller than that with fixed bias. On the other hand,

the system using fixed bias is simple and easy to implementation. In proposed system, fixed bias is used and has the bias value of $0.5s(t)$ that ensures nonnegative MSM signal to modulate an optical signal.

In the receiver shown in Fig. 1(a), the Gaussian noise is detected after the photo detector (PD). The converted electrical signal is divided into N 4-D receivers and demodulated with 4 orthogonal signals. In each 4-D receiver, 4 hard decision devices are used in obtaining a 4-D vector of detected symbol amplitudes $\boldsymbol{a}_i = (\hat{a}_{i1}, \hat{a}_{i2}, \hat{a}_{i3}, \hat{a}_{i4})$. The MLSD (maximum likelihood sequence detection) decoder regenerates the detected information bits $\hat{x}_1, ..., \hat{x}_k$.

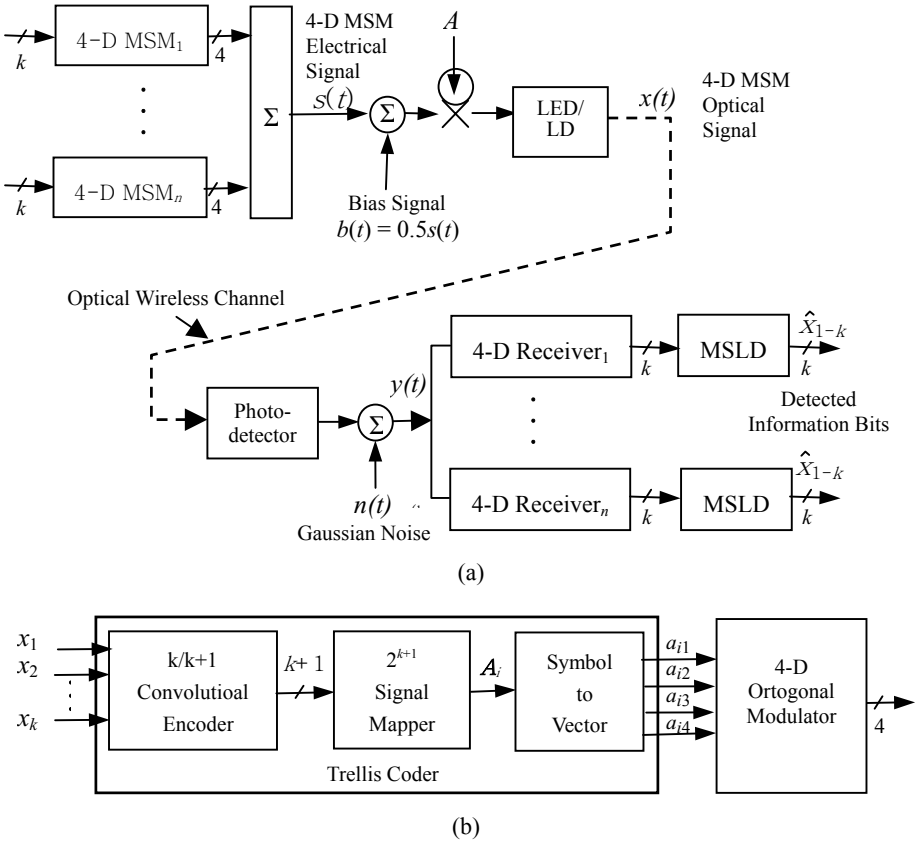

Fig. 1. MSM (Multiple–Subcarrier Modulation) system: (a) transmitter and receiver with 4-D orthogonal modulation scheme where n = 1, 2,…, N , and (b) 4-D trellis coder with orthogonal modulator. In the proposed system, the number of input bits k = 4 is used.

3 Generation of 4-D Vectors for the Proposed System

The error probability is almost entirely contributed by the nearest pair of signal points in an M-ary PSK scheme. For the case of high signal-to-noise ratio, we can choose a law of force expression, which can be given by [5].

$$\boldsymbol{F}_{ik} = C(k_0)e^{-|d_{ik}|^2/4k_0/T}\, d_{ik}/|d_{ik}| \tag{1}$$

where $\boldsymbol{F}_{ik}$ is the force between particle i and k, k_0 is the bandwidth of noise, and d_{ik} is the vector from particle i to particle k.

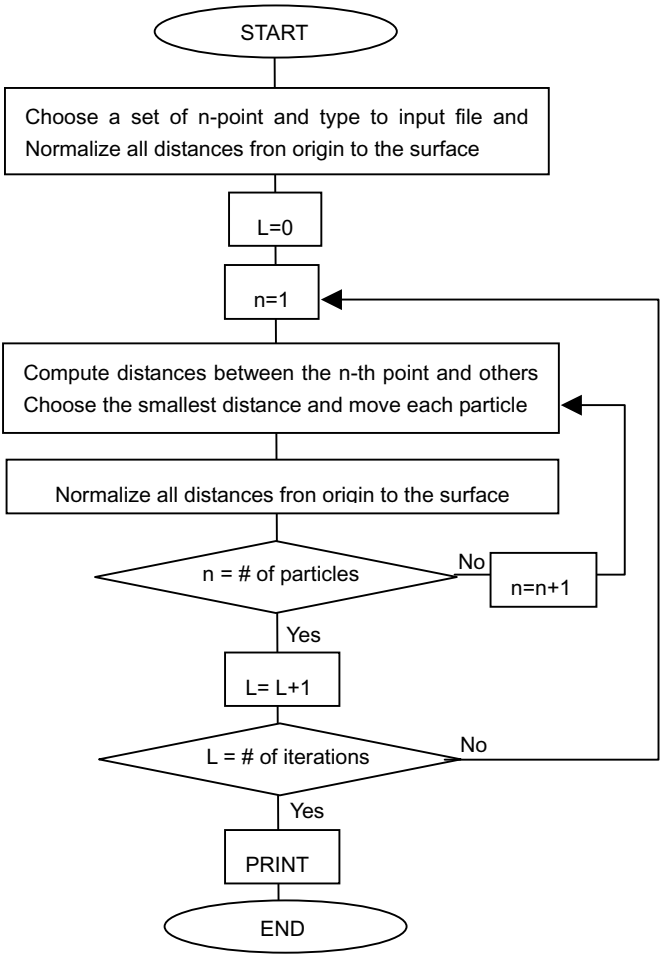

Fig. 2. The flowchart for the Problem

The program operates as the flowchart shown in Fig. 2 and has run for 32 points on the surface of a 4-D sphere. The results are shown in Table 1 where the symbols $\boldsymbol{A}_i$ are corresponding to output of 2^{k+1} signal mapper in Fig.1 (a) and the symmetric 4-D vectors are listed in an ascending order of the squared distances. The derived squared distance d^2 is 0 for A_1 itself, 0.8086 for A_1 to A_2, 3.8666 for A_1 to A_{32}, and so forth and the magnitude of each vector $|A_i| = \sqrt{a_{i1}^2 + a_{i2}^2 + a_{i3}^2 + a_{i4}^2} = 1$ so that this block code is symmetry and each 4-D symbol has the same energy as any other symbol with the minimum Euclidean distance. The signal number of each signal A_i is given in order to obtain the maximum subset distance for set partitioning of trellis coding that will be explained in Sect. 4.1. In the proposed system, 4-D vector, $\boldsymbol{a}_j = (a_{i1}, a_{i2}, a_{i3}, a_{i4})$, in Table 1 is used in transmitting 4 information bits for the block coder in Fig. 1(a).

4 Design of 16 State TCM

TCM has been developed actively, since the publication by Ungerboeck [6] appeared as a combined coding with modulation technique for digital transmission. The main advantage of TCM is the significant coding gain achieved over conventional uncoded modulation on the severely bandlimited additive white Gaussian noise channel while maintaining the same bandwidth and transmitted power.

In the proposed system, the number of input bits k is 4, so a rate 4/5 systematic convolutional encoder with feedback is used for the 16-state TCM schemes. In the trellis diagram, one of 16 possible signals listed in Table 2 is diverged from a trellis node because the number of input bit is four and one uncoded input bit x_1 provides parallel transitions of 2 signals.

In order to determine the minimum distance of a TCM scheme, set partitioning of the signals is necessary. 16 subsets which have different minimum squared distances in Table 2 are formed. Two signals in each subset are associated with parallel transitions, so that the minimum subset distance should be maximized. In order to obtain the maximum subset distances, after comparing all the distances between signal points, 16 subsets are chosen as shown in Table 2. Since the squared distance of each subset is greater than or equal to 3.459, the minimum squared distance associated with parallel transitions can be 3.459.

Without loss of generality, we choose the upper all-zero path to be correct and the lower path to be incorrect path that represents an error event as shown in Fig. 3. From the trellis in Fig. 3, the minimum squared distance of 16-state TCM scheme is d_m^2 = $0.809 \times 4 = 3.236$ because the distances associated with parallel transitions which are larger than this value.

Table 1. Computer derived 32-point vectors with maximized minimum squared distance on the surface of 4-D sphere

A_i	a_{i1}	a_{i2}	a_{i3}	a_{i4}	d^2 to A_1	Signal #
A_1	-0.362787	0.535530	0.077936	-0.758630	0.0000	0
A_2	-0.427980	-0.272260	0.466066	-0.724907	0.8086	1
A_3	0.451956	0.363509	-0.261169	-0.771614	0.8086	2
A_4	0.294727	0.241430	0.612178	-0.692882	0.8086	3
A_5	-0.691247	0.688544	-0.219103	0.008850	0.8086	4
A_6	-0.259356	0.371163	-0.753521	-0.476633	0.8086	5
A_7	-0.856946	-0.067417	-0.245302	-0.448248	0.8086	6
A_8	-0.116650	0.789680	0.591972	-0.111212	0.8086	7
A_9	0.156285	0.940721	-0.261711	-0.143747	0.9209	8
A_{10}	-0.181843	-0.018111	0.980102	-0.077489	1.6171	9
A_{11}	-0.701912	0.319009	0.513283	0.376952	1.6410	10
A_{12}	0.379311	-0.536620	0.171329	-0.734036	1.7095	11
A_{13}	0.773160	0.565435	0.271390	-0.094097	1.7703	12
A_{14}	0.283769	-0.376914	-0.688978	-0.550200	1.8822	26
A_{15}	-0.354732	-0.810617	-0.185695	-0.427296	1.9915	13
A_{16}	-0.787337	-0.502078	0.352972	0.058555	2.0003	28
A_{17}	-0.109646	0.770608	0.073873	0.623445	2.0295	27
A_{18}	0.527609	0.319783	-0.785662	-0.045853	2.0932	25
A_{19}	-0.407299	-0.368404	-0.835673	0.006029	2.2385	14
A_{20}	-0.815783	-0.052073	-0.288707	0.498432	2.2651	15
A_{21}	-0.192989	0.418606	-0.741856	0.487005	2.2662	19
A_{22}	0.935207	-0.175746	-0.187522	-0.243593	2.5264	31
A_{23}	0.333593	0.338596	0.716349	0.510795	2.5427	30
A_{24}	0.707852	-0.243788	0.660209	-0.060314	2.5803	20
A_{25}	0.014913	-0.810990	0.579961	-0.075618	2.6743	24
A_{26}	0.646590	0.374489	-0.208430	0.631059	3.0580	29
A_{27}	-0.200860	-0.359605	0.616925	0.670629	3.1608	21
A_{28}	0.430985	-0.877479	-0.210394	0.004127	3.2916	23
A_{29}	-0.289272	-0.774417	-0.168628	0.536810	3.4603	18
A_{30}	-0.075166	-0.021930	-0.143978	0.986478	3.4881	17
A_{31}	0.322350	-0.347136	-0.713213	0.516637	3.5007	16
A_{32}	0.581397	-0.433300	0.179701	0.664782	3.8666	22

Table 2. The Output Signal Sequences Diverged from Current States for 16 State TCM Scheme

Current state	Output Signals
0	(0, 16) (8, 24) (4, 20) (12, 28) (2, 18) (10, 26) (6, 22) (14, 30)
1	(1, 17) (9, 25) (5, 21) (13, 29) (3, 19) (11, 27) (7, 23) (15, 31)
2	(8, 24) (0, 16) (12, 28) (4, 20) (10, 26) (2, 18) (14, 30) (6, 22)
3	(9, 25) (1, 17) (13, 29) (5, 21) (11, 27) (3, 19) (15, 31) (7, 23)
4	(4, 20) (12, 28) (0, 16) (8, 24) (6, 22) (14, 30) (2, 18) (10, 26)
5	(5, 21) (13, 29) (1, 17) (9, 25) (7, 23) (15, 31) (3, 19) (11, 27)
6	(12, 28) (4, 20) (8, 24) (0, 16) (14, 30) (6, 22) (10, 26) (2, 18)
7	(13, 29) (5, 21) (9, 25) (1, 17) (15, 31) (7, 23) (11, 27) (3, 19)
8	(2, 18) (10, 26) (6, 22) (14, 30) (0, 16) (8, 24) (4, 20) (12, 28)
9	(3, 19) (11, 27) (7, 23) (15, 31) (1, 17) (9, 25) (5, 21) (13, 29)
10	(10, 26) (2, 18) (14, 30) (6, 22) (8, 24) (0, 16) (12, 28) (4, 20)
11	(11, 27) (3, 19) (15, 31) (7, 23) (9, 25) (1, 17) (13, 29) (5, 21)
12	(6, 22) (14, 30) (2, 18) (10, 26) (4, 20) (12, 28) (0, 16) (8, 24)
13	(7, 23) (15, 31) (3, 19) (11, 27) (5, 21) (13, 29) (1, 17) (9, 25)
14	(14, 30) (6, 22) (10, 26) (2, 18) (12, 28) (4, 20) (8, 24) (0, 16)
15	(15, 31) (7, 23) (11, 27) (3, 19) (13, 29) (5, 21) (9, 25) (1, 17)

5 Block Codes for the MSM System Using QPSK Scheme

For MSM systems, several block codes employing QPSK such as normal block code, reserved-subcarrier block code, and minimum-power block code to improve the power efficiency of an MSM optical communication system have been introduced [2].

Table 3. Set Partitioning of 32 Signals into 16 Subsets with $d^2 < 3.459$

Subset	Elements of Signals	Squared distance of subset
D_0	0, 16	3.500
D_1	1, 17	3.459
D_2	2, 18	3.565
D_3	3, 19	3.459
D_4	4, 20	3.605
D_5	5, 21	3.732
D_6	6, 22	3.622
D_7	7, 23	3.736
D_8	8, 24	3.802
D_9	9, 25	3.736
D_{10}	10, 26	3.761
D_{11}	11, 27	3.800
D_{12}	12, 28	3.605
D_{13}	13, 29	3.528
D_{14}	14, 30	3.712
D_{15}	15, 31	3.642

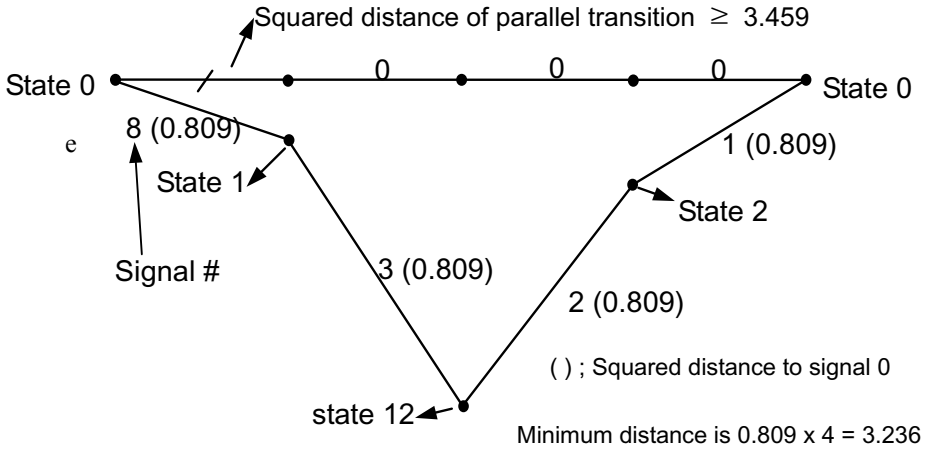

Fig. 3. The trellis to calculate the minimum distance of the 16 state TCM schem

Under the normal block coder, all N subcarriers are used for transmission of information bit where the number of input bits $k = 2N$, and the number of symbol $M = 2^{2N}$ for QPSK. Each information bit can be mapped independently to the corresponding symbol amplitudes. At the receiver, each detected symbol amplitude can be mapped independently to information bits.

Under the reserved-subcarrier block code, L subcarriers are reserved for minimizing the average optical power P. Hence, the number of input bits $k = 2(N\text{-}L)$, and the number of symbol $M = 2^{2(N\text{-}L)}$ for QPSK. An information bit vector is encoded by freely choosing the symbol amplitudes on the reserved subcarriers.

Under the minimum-power block code, no fixed set of subcarrier is reserved, but $L > 0$ subcarriers are reserved for the minimum value of the average optical power P. Also, the number of input bits $k = 2(N\text{-}L)$, and the number of symbol $M = 2^{2(N\text{-}L)}$ for QPSK and the average optical power always lower bounds the average optical power requirement.

6 Performance Evaluation

The power and bandwidth requirements of the proposed system are compared with that of the three block coders using QPSK scheme described in Sect. 5 as counterparts. For the MSM system with M-ary PSK including the proposed system and QPSK schemes, the signal is composed of a sum of modulated sinusoids so that the bit error probability can be [7]

$$P_b = Q\left(\sqrt{r^2 A^2 T / 2N_0}\right) \tag{2}$$

where T represents the rectangular pulse duration, r is the responsivity of photodetector in (1) and $Q(x)$ is the Gaussian error integral, and A is a nonnegative

scale factor. In the proposed system, one symbol is transmitted with 4 orthogonal subcarrier signals, while one symbol is transmitted with two subcarriers in QPSK. When we consider the number of input bits and subcarriers, N 4-D MSM system is equivalent to $2N$ x QPSK as described in Fig. 5. The error probability of each scheme is easily calculated with the minimum Euclidean distance. We set the required bit error probability to $P_b=10^{-6}$ [3].

Fig. 4 represents the numerical results of the normalized power requirement in optical dB versus the number of subcarriers with fixed bias for the proposed system and three block codes employing QPSK. Here, the normalized power requirements for three block codes employing QPSK are the results from [2] for fixed bias. The normalized power requirement of the proposed 4-D MSM is reduced up to 6.1 dB compared to those of above three block codes for QPSK scheme when the number of subcarriers is 4. For the number of subcarriers is 8, 12, and 16, the power requirement is reduced to 4.1 ~ 5.8 dB, 3.2 ~ 5.8 dB, and 2.8 ~ 5.8 dB, respectively. The power requirement in terms of the bandwidth requirement is also compared to measure the electrical bandwidth efficiency of the optical signal. Fig. 5 represents the normalized power requirement in optical dB versus the normalized bandwidth requirement with fixed bias for above three block codes employing QPSK and the proposed scheme. In the range of 1.125 ~ 1.5 of the normalized bandwidth requirement, the proposed system reduces up to 5.8 dB in bandwidth requirement. The proposed system has a large minimum value of 0.5s(t) and a large squared minimum distance of 3.236, so that the required dc bias is minimized and the error rate performance is improved. Hence, for wireless LAN using infrared communication, the proposed system can be much more efficient than the block codes using QPSK scheme for transmission of high-speed data with low power via the narrowband channel.

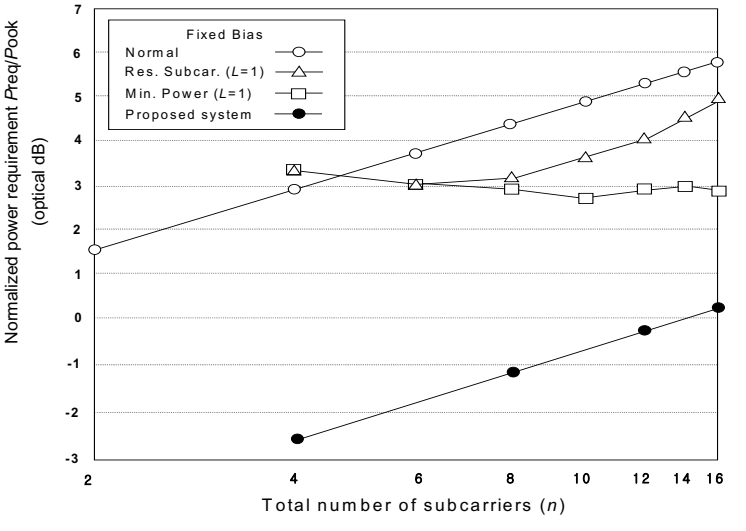

Fig. 4. Normalized power requirement versus total number of subcarriers for Normal QPSK, Res. Subcarrier, Min. Power, and the proposed 4-D MSM system

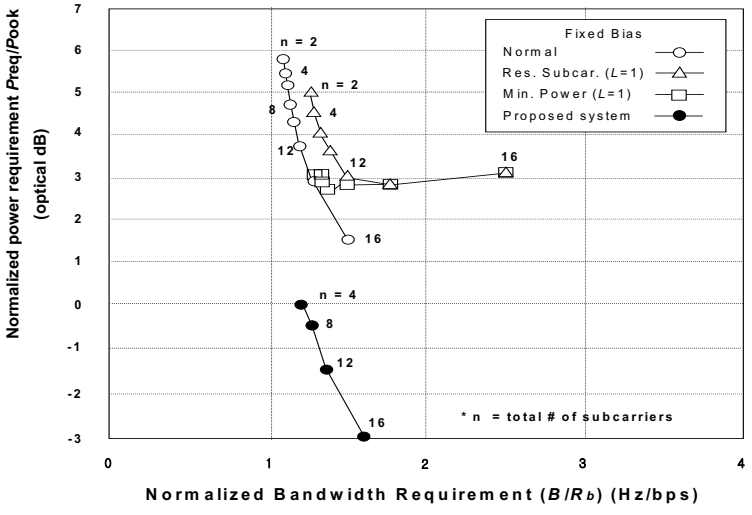

Fig. 5. Normalized power requirement versus normalized bandwidth requirement for Normal QPSK, Res. Subcarrier, Min. Power, and the proposed 4-D MSM system. Each number denotes total number of subcarriers.

7 Conclusions

This paper has described the basic principles and characteristics of multiple subcarrier modulation techniques in infrared communication for wireless LAN. The proposed system with the TCM scheme has a large squared minimum distance, so that the required dc bias is minimized and the error rate performance is improved. And, the optimization of signal waveform technique is used in deriving 4-D vectors for 32 points on the surface of Euclidean sphere having minimum distances between signal points. The 4-D MSM with fixed bias for optical wireless system using 4-D block coder improves the power and bandwidth efficiency, significantly. Hence, the proposed system needs much less power and bandwidth than the counterparts transmitting the same bit rates for optical wireless connection.

References

1. IEEE standard, http://standards.ieee.org/getieee802/802.11.html
2. Ohtsuki T.: Multiple-Subcarrier Modulation in Optical Wireless Communications. Vol. 3. IEEE Commun. Mag. (2003) 74-79
3. Kahn J., Berry J.: Wireless Infrared Communications. Vol. 2. Proc. IEEE (1997) 265-298
4. Teramoto S., Ohtsuki T.: Multiple-subcarrier Optical Communication System with Subcarrier Signal Point Sequence. IEEE GLOBECOM 2002

5. Lachs G.: Optimization of Signal Waveforms. Vol. 4. IEEE Trans. Information Theory (1963) 95-97
6. Ungerboeck G.: Channel Coding with Multilevel/Phase Signal. vol. IT-28. IEEE Trans. Information Theory (1982)
7. Hae Geun Kim: Trellis-Coded M-ary Orthogonal Modulation. IEEE Symposium on Computer and Communications. pp.364-367. 1995